PLANE WAVE SOLUTIONS AND MODAL ANALYSIS IN HIGHER ORDER SHEAR AND NORMAL DEFORMABLE PLATE THEORIES

R. C. Batra

Department of Engineering Science and Mechanics, M/C 0219, Virginia Polytechnic Institute and State University, Blacksburg, VA 24061, U.S.A.

AND

S. Vidoli AND F. Vestroni

Dipartimento di Ingegneria Strutturale e Geotecnica, Università di Roma "La Sapienza", 00184 Rome, Italy

We use the three-dimensional Hellinger–Reissner mixed variational principle to derive a Kth order ($K = 0, 1, 2, \ldots$) shear and normal deformable plate theory. The balance laws, the constitutive relations and the boundary conditions for the plate theory are deduced. The constitutive relations incorporate the shear and the normal tractions applied on the top and the bottom surfaces of the plate. For a Kth order plate theory with displacements expressed as a power series in the thickness co-ordinate z with terms up to z^K, the transverse shear and the transverse normal stresses involve terms upto z^{K+2} while in-plane stress components have terms up to z^K. The equations for the plate theory are expressed in a compact form by taking Legendre polynomials as the basis functions. The plate theory is used to study plane travelling waves and in particular the lengths of decay of the displacement components; this allows for a rigorous ordering of the importance of the displacement descriptors in terms of decaying properties.

Finally, we study the free vibrations of a simply supported rectangular orthotropic thick plate; results from the present theory are compared with an exact three-dimensional solution and with other plate theories. To this end, a Kth order compatible plate theory is also deduced; the term "compatible" alludes to the fact that the reduction map for the stress fields is induced by the kinematical reduction map, whilst in the "mixed" models it is postulated independently. It is found that the frequencies up to the fifth mode of vibration computed with the fifth order theory and without introducing any shear correction factors match very well with the corresponding analytical solution. Also, through-the-thickness distribution of all of the stress components is found to agree well with the three-dimensional elasticity solution, while the stress distribution obtained from the compatible plate theories deviates considerably, especially for the higher modes.

1. INTRODUCTION

Most of the higher order plate theories available in the literature neglect transverse normal strains, those due to Mindlin and Medick [1], Soldatos and Watson [2], Babu and Kant [3], Chao *et al.* [4], Lee and Yu [5], Batra and Vidoli [6], Messina [7], Carrera [8], Di Carlo *et al.* [9] and the Cosserat brothers [10], amongst others, account for them. In general, all these plate theories are derived from the equations of three-dimensional

elasticity by expanding the kinetic and the kinematic fields as a power series in terms of the thickness co-ordinate z, and the plate theory is called higher order if terms involving z^K with $K \geqslant 3$ are retained in these expansions. A challenging task is to investigate the least value of K so that the derived plate theory is manageable and, at the same time, accurate. The optimal value of K depends upon the aspect ratio of the plate, the boundary conditions prescribed at its edges, the applied loads and which aspects of the three-dimensional deformations should be more accurately modelled.

Several approaches are possible in deriving the equations of a shell or plate model. Here a "deductive" method is used: by using Legendre polynomials in z as the basis functions and the mixed Hellinger–Reissner variational principle, we derive from the three-dimensional elasticity a mixed Kth order plate theory that is easily amenable to analysis. It accounts for both transverse shear and transverse normal deformations of the plate, and boundary conditions of normal and tangential tractions prescribed on its top and bottom surfaces are exactly satisfied through the proposed constitutive relations. We use this theory to study plane travelling waves in a transversely isotropic plate and to order the displacement descriptors introduced in terms of their decaying properties: the fastest a wave dominated by a given displacement component decays, the less its contribution to the overall motion of the plate. Furthermore, a theorem on the decomposition of plane waves in a Kth order plate is stated; these can be split into four uncoupled types: transverse symmetric, transverse skew-symmetric, longitudinal membranal and longitudinal flexural.

Finally, frequencies of a simply supported homogeneous orthotropic rectangular plate found with the fifth order theory match exactly with the analytical solution of Srinivas and Rao [11]. Also, through-the-thickness variations of different stress components computed from the plate theory agree well with those obtained from the solution of the three-dimensional elasticity equations. These results are also compared with results from the Kirchhoff and Mindlin models and from compatible plate theories; these last refer to higher order shear and normal deformable plate theories whose constitutive relations are obtained through a minimization of the standard energy functional; the reduction map for the stresses are, in this case, simpler and do not satisfy the boundary conditions on the upper and lower surfaces of the plate.

2. FORMULATION OF THE PROBLEM

Consider a prismatic anisotropic linear elastic body occupying the region $\mathscr{C} = \mathscr{S} \times \mathscr{I}$, where $\mathscr{S} \subset \mathscr{R}^2$ is a plane surface and $\mathscr{I}$ is the real interval $[-h, h]$. The boundary of $\mathscr{C}$ can be written as

$$\partial \mathscr{C} = (\partial \mathscr{S} \times \mathscr{I}) \cup \mathscr{S}^+ \cup \mathscr{S}^-$$

where $\partial \mathscr{S}$ is the periphery of $\mathscr{S}$, and $\mathscr{S}^+$ and $\mathscr{S}^-$ the top and the bottom surfaces of $\mathscr{C}$, i.e., $\mathscr{S}^+ = \mathscr{S} \times \{h\}$, and $\mathscr{S}^- = \mathscr{S} \times \{-h\}$. $\mathscr{M} = \partial \mathscr{S} \times \mathscr{I}$ is called the mantle or the edges of $\mathscr{C}$. For a rectangular plate, $\mathscr{S}$ equals the rectangular region occupied by the midsurface of the plate and $\mathscr{M}$ the four edges.

Equations governing deformations of an elastic body can be found as a saddle point of the Hellinger–Reissner mixed functional

$$\mathfrak{H}(\mathbf{u}, \mathbf{S}) = \int_{\partial_d \mathscr{C}} \mathbf{Sn} \cdot (\mathbf{u} - \bar{\mathbf{u}}) + \int_{\partial_b \mathscr{C}} \mathbf{t} \cdot \mathbf{u} + \int_{\mathscr{C}} (\mathbf{b} \cdot \mathbf{u} - \mathbf{S} \cdot \mathbf{E}(\mathbf{u}) + \tfrac{1}{2} \mathbf{S} \cdot \mathbb{F} \mathbf{S}). \tag{1}$$

Here $\mathbf{u}$ is the displacement of a point, $\mathbf{E}(\mathbf{u}) = [\text{Grad } \mathbf{u} + (\text{Grad } \mathbf{u})^{\mathrm{T}}]/2$ the infinitesimal strain tensor, Grad the three-dimensional gradient operator, $\mathbf{t} = \mathbf{S}\mathbf{n}$ the surface traction, $\mathbf{n}$ an outward unit normal to the boundary, $\mathbf{S}$ the stress tensor, $\mathbf{b}$ the body force and $\mathbb{F}$ is the fourth order compliance tensor. Moreover

$$\partial_a \mathscr{C} \cup \partial_b \mathscr{C} = \partial \mathscr{C}, \qquad \partial_a \mathscr{C} \cap \partial_b \mathscr{C} = \emptyset,$$

where $\partial_a \mathscr{C}$ and $\partial_b \mathscr{C}$ are the surfaces on which, respectively, the displacement $\mathbf{u}$ is prescribed as $\bar{\mathbf{u}}$ and the surface traction $\mathbf{S}\mathbf{n}$ as $\mathbf{t}$. To save some writing, the variable of integration has been omitted in all integrals; the specified domain of integration indicates whether it is an area, a volume or a line integral. When studying dynamic deformations, the body force $\mathbf{b}$ is replaced by $\mathbf{b}^{(a)} - \rho\ddot{\mathbf{u}}$, where $\mathbf{b}^{(a)}$ is the externally applied body force, ρ the mass density and a superimposed dot indicates partial differentiation with respect to time.

The variation of $\mathfrak{H}$ with respect to the displacement field $\mathbf{u}$ gives the balance equations and the essential boundary conditions, while its variation with respect to the stress field $\mathbf{S}$ provides the constitutive relations and the natural boundary conditions.

We use the following decomposition of the position vector $\mathbf{x}$, the displacement field $\mathbf{u}$ and the outward unit normal $\mathbf{n}$:

$$\mathbf{x} = \mathbf{r} + z\,\mathbf{e}, \qquad \mathbf{u} = \mathbf{v} + w\,\mathbf{e}, \qquad \mathbf{n} = \hat{\mathbf{n}} + n\,\mathbf{e}, \tag{2}$$

where $\mathbf{e}$ is the unit normal to $\mathscr{S}$. Thus $\mathbf{v}$ and w denote, respectively, the displacement of a point within and perpendicular to $\mathscr{S}$. The other field variables can now be written as

$$\mathbf{E}(\mathbf{u}) = \text{sym grad } \mathbf{v} + \frac{\mathbf{v}' + \text{grad } w}{2} \otimes \mathbf{e} + \mathbf{e} \otimes \frac{\mathbf{v}' + \text{grad } w}{2} + w'\mathbf{e} \otimes \mathbf{e}$$

$$=: \hat{\mathbf{E}} + \boldsymbol{\gamma} \otimes \mathbf{e} + \mathbf{e} \otimes \boldsymbol{\gamma} + \varepsilon\,\mathbf{e} \otimes \mathbf{e},$$

$$\mathbf{S} = \hat{\mathbf{S}} + \mathbf{s} \otimes \mathbf{e} + \mathbf{e} \otimes \mathbf{s} + \sigma\,\mathbf{e} \otimes \mathbf{e}, \qquad \mathbf{b} = \hat{\mathbf{b}} + \beta\,\mathbf{e}, \qquad \mathbf{t} = \hat{\mathbf{t}} + t\,\mathbf{e}, \tag{3}$$

and the constitutive relations are partitioned as

$$\begin{Bmatrix} \hat{\mathbf{E}} \\ \boldsymbol{\gamma} \\ \varepsilon \end{Bmatrix} = \begin{bmatrix} \mathbb{H} & \mathbb{M} & \mathbb{N} \\ \mathbb{M}^{\top} & \mathbb{G} & \mathbb{L} \\ \mathbb{N}^{\top} & \mathbb{L}^{\top} & \mathbb{E} \end{bmatrix} \begin{Bmatrix} \hat{\mathbf{S}} \\ \mathbf{s} \\ \sigma \end{Bmatrix}, \tag{4}$$

where $w' = \partial w/\partial z$, grad is the two-dimensional gradient operator, sym grad $\mathbf{v} = (\text{grad } \mathbf{v} + (\text{grad } \mathbf{v})^{\mathrm{T}})/2$. Furthermore, $\hat{\mathbf{E}}$ represents the in-plane strain tensor, $\hat{\mathbf{S}}$ the in-plane stress tensor, $\boldsymbol{\gamma}$ the transverse shear strain, $\mathbf{s}$ the transverse shear stress, ε the transverse normal strain and σ the transverse normal stress. $\mathbf{a} \otimes \mathbf{b}$ equals the tensor product between vectors $\mathbf{a}$ and $\mathbf{b}$; and $(\mathbf{a} \otimes \mathbf{b})\mathbf{c} = (\mathbf{b} \cdot \mathbf{c})\mathbf{a}$ for every vector $\mathbf{c}$. Here $\hat{\mathbf{E}}$ and $\hat{\mathbf{S}}$ are three-dimensional vectors, $\boldsymbol{\gamma}$ and $\mathbf{s}$ two-dimensional vectors, and ε and σ are scalars. Furthermore, $\mathbb{H}$, $\mathbb{G}$ and $\mathbb{M}$, $\mathbb{N}$, $\mathbb{L}$, $\mathbb{E}$ are respectively 3×3, 2×2 symmetric and 3×2, 3×1, 2×1, 1×1 matrices. The forms of these matrices for a transversely isotropic material are given in section 3.2. In terms of the quantities introduced in equations (2)–(4), Hellinger–Reissner functional (1) becomes

$$\mathfrak{H}(\mathbf{v}, w, \hat{\mathbf{S}}, \mathbf{s}, \sigma) = \int_{\mathscr{C}} [(\hat{\mathbf{b}} \cdot \mathbf{v} + \beta\,w) - (\hat{\mathbf{S}} \cdot \hat{\mathbf{E}} + 2\mathbf{s} \cdot \boldsymbol{\gamma} + \sigma\varepsilon)] + \int_{\partial_b \mathscr{C}} (\hat{\mathbf{t}} \cdot \mathbf{v} + tw)$$

$$+ \int_{\partial_a \mathscr{C}} [(\hat{\mathbf{S}}\hat{\mathbf{n}} + \mathbf{s}\,n) \cdot (\mathbf{v} - \bar{\mathbf{v}}) + (\mathbf{s} \cdot \hat{\mathbf{n}} + \sigma n)(w - \bar{w})]$$

$$\rightarrow \frac{1}{2} \int_{\mathscr{C}} [\hat{\mathbf{S}} \cdot (\mathbb{H}\hat{\mathbf{S}} + \mathbb{M}\mathbf{s} + \mathbb{N}\sigma) + \mathbf{s} \cdot (\mathbb{M}^{\top}\hat{\mathbf{S}} + \mathbb{G}\mathbf{s} + \mathbb{L}\sigma) + \sigma(\mathbb{N}^{\top}\hat{\mathbf{S}} + \mathbb{L}^{\top}\mathbf{s} + \mathbb{E}\sigma)]. \tag{5}$$

3. TWO HIGHER ORDER PLATE THEORIES

3.1. MIXED HIGHER ORDER PLATE THEORY (M)

For a plate-like body, displacements are usually not prescribed on its top surface $\mathscr{S}^+$ and the bottom surface $\mathscr{S}^-$. However, displacements and/or surface tractions may be prescribed on the mantle or the edges of the plate. Thus

$$\partial_a \mathscr{C} = \mathscr{M}_a, \quad \partial_b \mathscr{C} = \mathscr{M}_b \cup \mathscr{S}^+ \cup \mathscr{S}^-,$$

where $\mathscr{M}_a$ and $\mathscr{M}_b$ are parts of the mantle $\mathscr{M}$ where displacements and surface tractions are prescribed respectively. Let

$$L_0(z) = \frac{1}{\sqrt{2h}}, \quad L_1(z) = \sqrt{\frac{3}{2h}}\frac{z}{h}, \quad L_2(z) = \sqrt{\frac{5}{2h}}\left(3\frac{z^2}{h^2} - 1\right)\Big/2,$$

$$L_3(z) = \sqrt{\frac{7}{2h}}\left(-\frac{3}{2}\frac{z}{h} + \frac{5}{2}\frac{z^3}{h^3}\right), \ldots \tag{6}$$

represent Legendre polynomials defined on $[-h, h]$, and normalized as

$$\langle L_i, L_j \rangle := \int_{-h}^{h} L_i(z)\,L_j(z)\,\mathrm{d}z = \delta_{ij}, \quad i, j = 0, 1, 2, \ldots, K, \tag{7}$$

where δ_{ij} is the Kronecker delta. The displacement fields $\mathbf{v}$ and w are expanded as

$$\mathbf{v}(\mathbf{r}, z) = L_i(z)\,\mathbf{v}_i(\mathbf{r}), \quad w(\mathbf{r}, z) = L_i(z)\,w_i(\mathbf{r}). \tag{8}$$

Here and below a repeated index implies summation over the range of the index. Components of the displacements v_i and w_i for $K = 3$ are plotted in Figure 1.

For displacements given by equation (8), we have

$$\hat{\mathbf{E}} = L_i(z)\,\text{sym grad}\,\mathbf{v}_i =: L_i(z)\,\hat{\mathbf{E}}_i,$$

$$\gamma = L_i(z)\left(\frac{D_{ji}\mathbf{v}_j + \text{grad}\,w_i}{2}\right) =: L_i(z)\gamma_i, \tag{9}$$

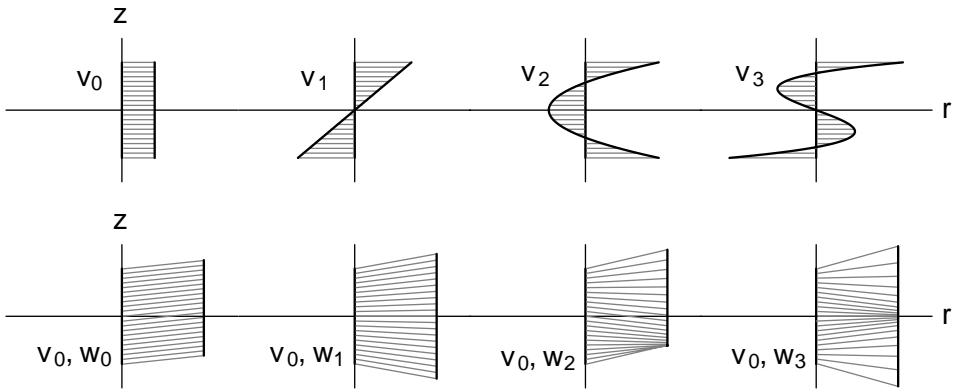$$\varepsilon = L_i(z)\,D_{ji}\,w_j =: L_i(z)\varepsilon_i,$$

Figure 1. Components of displacements for a third order plate theory.

where we have set

$$L_i'(z) = D_{ij} L_j(z) \tag{10}$$

and D_{ij} are constants. Note that the first row and the last column of the $(K + 1) \times (K + 1)$ matrix D_{ij} are identically zero, since differentation of a Kth order polynomial yields a polynomial of order $(K - 1)$. This has consequences in the balance equations where, for instance, the shear force does not appear in the balance of the membranal stress tensor while it does appear in the balance of bending moments; see equations (15).

The functional $\mathfrak{H}$ given in equation (5) now reduces to

$$\mathfrak{H} = \int_{\mathscr{S}} (\mathbf{B}_i \cdot \mathbf{v}_i + \varXi_i w_i) + \int_{\partial_b \mathscr{S}} [(\mathbf{F}_i - \mathbf{N}_i \hat{\mathbf{n}}) \cdot \mathbf{v}_i + (\varPhi_i - \mathbf{T}_i \cdot \hat{\mathbf{n}}) w_i]$$

$$+ \int_{\mathscr{S}} [(\operatorname{div} \mathbf{N}_i - D_{ji} \mathbf{T}_j) \cdot \mathbf{v}_i + (\operatorname{div} \mathbf{T}_i - D_{ji} \varSigma_j) w_i] + \mathfrak{R}(\hat{\mathbf{S}}, \mathbf{s}, \sigma), \tag{11}$$

where

$$\mathbf{B}_i = \langle L_i, \hat{\mathbf{b}} \rangle + L_i(h) \hat{\mathbf{t}}^+ + L_i(-h) \hat{\mathbf{t}}^-, \quad \mathbf{F}_i = \langle L_i, \hat{\mathbf{t}} \rangle,$$

$$\varXi_i = \langle L_i, \beta \rangle + L_i(h) t^+ + L_i(-h) t^-, \quad \varPhi_i = \langle L_i, t \rangle, \tag{12}$$

$$\mathbf{N}_i = \langle L_i, \hat{\mathbf{S}} \rangle, \quad \mathbf{T}_i = \langle L_i, \mathbf{s} \rangle, \quad \varSigma_i = \langle L_i, \sigma \rangle,$$

div is the two-dimensional divergence operator, and $\mathfrak{R}(\hat{\mathbf{S}}, \mathbf{s}, \sigma)$ is the part of $\mathfrak{H}$ that does not depend upon the displacements. Superscripts $+$ and $-$ on a quantity signify its values on surfaces $\mathscr{S}^+$ and $\mathscr{S}^-$ respectively. Furthermore, $\mathbf{N}_i$ is a 2×2 symmetric matrix; $\mathbf{N}_0$ gives the in-plane (within the plane $\mathscr{S}$) forces and is sometimes called the membranal stress tensor, $\mathbf{N}_1$ is the matrix of bending moments also called the moment tensor, the matrix $\mathbf{N}_i$ $(i = 2, 3, \dots, K)$ is comprised of a linear combination of matrices of bending moments of order zero through i, $\mathbf{T}_0$ is the resultant shear force or the shear stress vector, $\mathbf{T}_1$ is the moment of the internal double forces (i.e., forces acting along the normal $\mathbf{e}$ to the midsurface of the plate), $\mathbf{T}_i$ $(i = 2, 3, \dots, K)$ equals the linear combination of moments up to the ith order of the internal double forces, $\varSigma_0$ is the transverse normal force, and $\varSigma_i$ $(i = 1, 2, 3, \dots, K)$ the linear combination of the moments up to the ith order of the transverse normal force. Note that the tangential and the normal surface tractions applied on the top and the bottom surfaces of the plate appear in the definitions of $\mathbf{B}_i$ and $\varXi_i$. Because of the relation $L_i(-h) = (-1)^i L_i(h)$ in which the index i is not summed,

$$L_i(h) t^+ + L_i(-h) t^- = \begin{cases} L_i(h)(t^+ + t^-), & i = 0, 2, 4, \dots, \\ L_i(h)(t^+ - t^-), & i = 1, 3, 5, \dots, \end{cases}$$

and similar relations hold for $\hat{\mathbf{t}}$.

If the body forces include the inertia forces, i.e.,

$$\mathbf{b} = \mathbf{b}^{(a)} - \rho \ddot{\mathbf{u}}, \tag{13}$$

then

$$\mathbf{B}_i = \mathbf{B}_i^{(a)} - R_{ij} \ddot{\mathbf{v}}_j, \qquad \varXi_i = \varXi_i^{(a)} - R_{ij} \ddot{w}_j, \tag{14}$$

where $R_{ij} = \langle \rho L_i, L_j \rangle$. If the mass density ρ is independent of z, then $R_{ij} = \rho \, \delta_{ij}$.

The variation of $\mathfrak{H}$ with respect to $\mathbf{v}_i$ and w_i gives

$$\begin{aligned} \text{div } \mathbf{N}_i - D_{ij}\mathbf{T}_j + \mathbf{B}_i^{(a)} &= R_{ij}\ddot{\mathbf{v}}_j, \\ \text{div } \mathbf{T}_i - D_{ij}\Sigma_j + \Xi_i^{(a)} &= R_{ij}\ddot{w}_j, \end{aligned} \quad \text{on } \mathscr{S}, \tag{15}$$

$$\begin{aligned} \mathbf{N}_i\hat{\mathbf{n}} &= \mathbf{F}_i, \\ \mathbf{T}_i\cdot\hat{\mathbf{n}} &= \Phi_i, \end{aligned} \quad \text{on } \partial_b\mathscr{S}, \quad i = 0, 1, 2, \dots, K. \tag{16}$$

These are the balance equations and the natural boundary conditions for the plate theory. Equations $(15)_1$ and $(15)_2$ are coupled because of the presence of the moments $\mathbf{T}_i$ in both equations. Recalling that the matrix D_{ij} is non-diagonal, $\mathbf{T}_0, \mathbf{T}_1, \dots, \mathbf{T}_K$ and $\Sigma_0, \Sigma_1, \dots, \Sigma_K$ will appear in equations $(15)_1$ and $(15)_2$ respectively. Thus in order to solve the problem for the Kth order theory, the $2(K+1)$ equations (15) need to be solved simultaneously.

A mixed variational principle requires an Ansatz for the expansion of stress fields in the thickness direction. We choose an expansion that automatically satisfies equations $(12)_{5,6,7}$ and the boundary conditions

$$\mathbf{s}(\mathbf{r}, \pm h) = \pm \hat{\mathbf{t}}^{\pm}, \qquad \sigma(\mathbf{r}, \pm h) = \pm t^{\pm}, \tag{17}$$

on the top and the bottom surfaces of the plate. To this end we set

$$\hat{\mathbf{S}}(\mathbf{r}, z) = L_i(z)\mathbf{N}_i(\mathbf{r}),$$

$$\mathbf{s}(\mathbf{r}, z) = \tilde{L}_i(z)\mathbf{T}_i(\mathbf{r}) + \alpha_0[L_0(z) - \tilde{L}_0(z)]\hat{\mathbf{t}}_0(\mathbf{r}) + \alpha_1[L_1(z) - \tilde{L}_1(z)]\hat{\mathbf{t}}_1(\mathbf{r}), \tag{18}$$

$$\sigma(\mathbf{r}, z) = \tilde{L}_i(z)\Sigma_i(\mathbf{r}) + \alpha_0[L_0(z) - \tilde{L}_0(z)]t_0(\mathbf{r}) + \alpha_1[L_1(z) - \tilde{L}_1(z)]t_1(\mathbf{r}),$$

where

$$\hat{\mathbf{t}}_0(\mathbf{r}) = (\hat{\mathbf{t}}^+ - \hat{\mathbf{t}}^-)/2, \qquad \hat{\mathbf{t}}_1(\mathbf{r}) = (\hat{\mathbf{t}}^+ + \hat{\mathbf{t}}^-)/2,$$

$$t_0(\mathbf{r}) = (t^+ - t^-)/2, \qquad t_1(\mathbf{r}) = (t^+ + t^-)/2, \tag{19}$$

$$\alpha_0 = 1/L_0(h), \qquad \alpha_1 = 1/L_1(h), \tag{20}$$

$$\langle \tilde{L}_i, L_j \rangle = \delta_{ij}, \qquad \tilde{L}_i(\pm h) = 0, \qquad i, j = 0, 1, 2, \dots, K. \tag{21}$$

Thus the in-plane stresses, $\hat{\mathbf{S}}$, are expressed as a polynomial in z of degree K, but the transverse shear stresses and the transverse normal stress as polynomials of degree $K + 2$ in z. Note that, for $z = \pm h$, $\mathbf{s}$ and σ automatically satisfy all the boundary conditions (17). The $\tilde{L}_i(z)$ are Legendre polynomials of degree $(K + 2)$; they are not only orthogonal to all $L_j(z)$, $j \neq i$ but must also vanish at $z = \pm h$ so that traction boundary conditions on the top and the bottom surfaces of the plate are exactly satisfied by the last two terms of equations $(18)_2$ and $(18)_3$. They can be uniquely computed through equation (21). For $K = 3$, the solution of equations $(21)_1$ and $(21)_2$ is

$$\tilde{L}_0(z) = \tfrac{\sqrt{2}}{16}(5 + 30(\tfrac{z}{h})^2 - 35(\tfrac{z}{h})^4),$$

$$\tilde{L}_1(z) = \tfrac{1}{16}\sqrt{\tfrac{2}{3}}(-21\tfrac{z}{h} + 210(\tfrac{z}{h})^3 - 189(\tfrac{z}{h})^5),$$

$$\tilde{L}_2(z) = \tfrac{1}{10}\sqrt{\tfrac{2}{5}}(-35 + 210(\tfrac{z}{h})^2 - 175(\tfrac{z}{h})^4),$$

$$\tilde{L}_3(z) = \tfrac{1}{16}\sqrt{\tfrac{2}{7}}(-187\tfrac{z}{h} + 630(\tfrac{z}{h})^3 - 441(\tfrac{z}{h})^5). \tag{22}$$
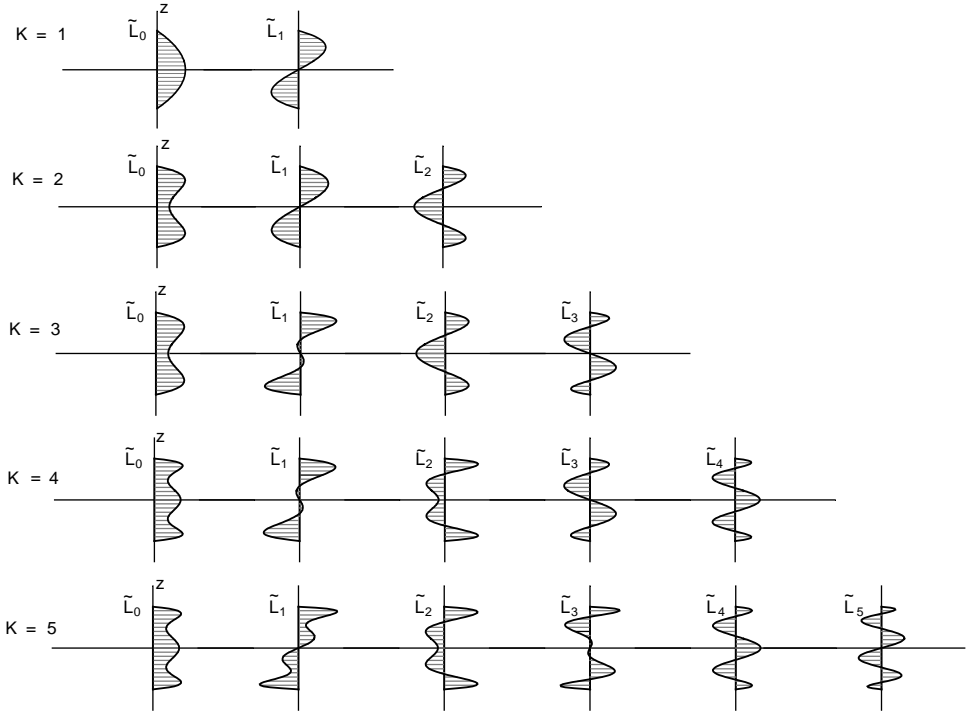
Figure 2. Plots of the polynomial bases $\tilde{L}_i$ used in the representations of the transverse shear and the transverse normal stresses for $K = 1, 2, 3, 4$ and 5.

Expressions for these functions for $K = 1, 2, \ldots, 7$ are given in reference [6]. For K ranging from 1 to 5, the polynomial $\tilde{L}_i(z)$ is plotted in the $(i + 1)$th column of Figure 2. Note that each $\tilde{L}_i(z)$ depends on the order K of the theory; however, the polynomials in each row contain the polynomials of the following row. For instance, the parabolic distribution represented by $\tilde{L}_0$ for $K = 1$ in the first row can be represented as a linear combination of the z-even polynomials in the second row, namely $\tilde{L}_{0, K=2}$ and $\tilde{L}_{2, K=2}$. We also remark that these polynomials, as well as their inner products, can be computed exactly, i.e., without any numerical approximation, for every order K.

Substitution from equation (18) into equation (5) and setting the variation of $\mathfrak{H}$ with respect to $\mathbf{N}_i, \mathbf{T}_i$, and Σ_i gives the constitutive relations

$$\begin{Bmatrix} \hat{\mathbf{E}}_i \\ \gamma_i \\ \varepsilon_i \end{Bmatrix} = \begin{pmatrix} \mathbb{H}_{ij} & \mathbb{M}_{ij} & \mathbb{N}_{ij} \\ \mathbb{M}_{ij}^\top & \mathbb{G}_{ij} & \mathbb{L}_{ij} \\ \mathbb{N}_{ij}^\top & \mathbb{L}_{ij}^\top & \mathbb{E}_{ij} \end{pmatrix} \begin{Bmatrix} \mathbf{N}_j \\ \mathbf{T}_j \\ \Sigma_j \end{Bmatrix} + \begin{Bmatrix} \mathbf{0} \\ (\delta_{ij} - P_{ij}) \alpha_j (\mathbb{G}\, \hat{\mathbf{t}}_i + \mathbb{L}\, t_i) \\ (\delta_{ij} - P_{ij}) \alpha_j (\mathbb{L}^\top \hat{\mathbf{t}}_i + \mathbb{E}\, t_i) \end{Bmatrix} \qquad (23)$$

and the essential boundary conditions

$$\mathbf{v}_i = \tilde{\tilde{\mathbf{v}}}_i, \quad w_i = \tilde{\tilde{w}}_i, \quad \text{on } \partial_a \mathscr{S}, \qquad (24)$$

where $\alpha_j = 0$ for $j \geqslant 2$, and

$$\begin{aligned} \mathbb{H}_{ij} &= \langle \mathbb{H} L_i, L_j \rangle, & \mathbb{M}_{ij} &= \langle \mathbb{M} L_i, \tilde{L}_j \rangle, & \mathbb{N}_{ij} &= \langle \mathbb{N} L_i, \tilde{L}_j \rangle, \\ \mathbb{G}_{ij} &= \langle \mathbb{G} \tilde{L}_i, \tilde{L}_j \rangle, & \mathbb{L}_{ij} &= \langle \mathbb{L}\, \tilde{L}_i, \tilde{L}_j \rangle, & \mathbb{E}_{ij} &= [\mathbb{E} \tilde{L}_i, \tilde{L}_j \rangle, \\ P_{ij} &= \langle \tilde{L}_i, \tilde{L}_j \rangle, & \bar{\mathbf{v}}_i &= \langle L_i, \bar{\mathbf{v}} \rangle, & \tilde{w}_i &= \langle \tilde{L}_i, \bar{w} \rangle, & i, j = 0, 1, 2, \ldots, K. \end{aligned} \qquad (25)$$

In the second term on the right-hand side of equation (23), the index i is not summed. For a homogeneous plate, or when the material properties do not vary in the thickness direction, $\mathbb{H}_{ij} = \mathbb{H}\delta_{ij}$, etc.

Balance laws (15), constitutive relations (23), boundary conditions (16) and (24) and the strain–displacement relations (9) form a complete set of equations for the Kth order shear and normal deformable plate theory. For $K = 1$ and 3, the present plate theory differs from the first order shear deformation theory (FSDT) and the third order shear deformation theory (TSDT) at least in the following two respects. Whereas these theories assume that both the transverse normal strain and the transverse normal stress vanish identically, we do not; as a matter of fact, the simultaneous vanishing of the transverse normal strain and the transverse normal stress is mutually incompatible. Also, in the FSDT and the TSDT, the transverse shear stresses are taken to be polynomials of degree 0 and 2 respectively. Here these stresses are expressed as polynomials of degree 3 and 5 respectively. We note that in the derivation of the TSDT, Reddy [12] and Hanna and Leissa [13] required that the tangential tractions identically vanish on the top and the bottom surfaces of the plate. The present plate theory accounts for non-zero tangential tractions applied on the top and/or the bottom surface of the plate.

Results obtained from this theory are identified with the letter M to signify the use of the mixed variational principle in the derivation of the theory.

3.2. A COMPATIBLE HIGHER ORDER PLATE THEORY (C)

Mindlin and Medick [1], following the suggestion of W. Prager, also used Legendre polynomials to expand the displacements as an infinite power series in z, substituted expressions (9) for strains in the constitutive relation $\mathbf{S} = \mathbb{F}^{-1}\mathbf{E}$, and employed the principle of virtual work to derive the constitutive relations for stress resultants and moments of the plate theory. This kind of procedure is called "compatible" since, after having defined the kinematical reduction map (8), the reduction map for stresses is based on the same set of polynomial functions and is only constrained to satisfy equations $(12)_{5,6,7}$ induced by the kinematical reduction map (8); the only functional needed, in this case, is represented by the principle of virtual power. In the literature several authors have used "compatible" identification procedures both for deducing plate or beam equations or to implement finite element codes; see for instance reference [14].

In order to compare results with our model, we here sketch the compatible identification procedure for a Kth order plate; it consists in substituting for $\hat{\mathbf{E}}$, $\boldsymbol{\gamma}$ and ε from equations (9) into equation (4), solving it for $\hat{\mathbf{S}}$, $\mathbf{s}$ and σ, and then use definitions $(12)_{5,6,7}$ of $\mathbf{N}_i$, $\mathbf{T}_i$ and Σ_i to derive expressions for them in terms of the displacements. We call the so derived plate theory a compatible higher order shear and normal deformable plate theory, and signify results computed from it by the letter C.

Assuming that constitutive relation (4) is invertible, we write its inverse as

$$\begin{Bmatrix} \hat{\mathbf{S}} \\ \mathbf{s} \\ \sigma \end{Bmatrix} = \begin{bmatrix} \mathbb{A} & \mathbb{Q} & \mathbb{F} \\ \mathbb{Q}^\top & \mathbb{B} & \mathbb{R} \\ \mathbb{F}^\top & \mathbb{R}^\top & \mathbb{C} \end{bmatrix} \begin{Bmatrix} \hat{\mathbf{E}} \\ \boldsymbol{\gamma} \\ \varepsilon \end{Bmatrix} \tag{26}$$

and, substituting for stresses into definition $(12)_{5,6,7}$ of $\mathbf{N}_i$, $\mathbf{T}_i$ and Σ_i and for strains from equation (9), we get

$$\mathbf{N}_i = \langle L_i, \hat{\mathbf{S}} \rangle = \langle L_i, L_j \mathbb{A} \rangle \hat{\mathbf{E}}_j + \langle L_i, L_j \mathbb{Q} \rangle \boldsymbol{\gamma}_j + \langle L_i, L_j \mathbb{F} \rangle \varepsilon_j,$$

$$\mathbf{T}_i = \langle L_i, \mathbf{s} \rangle = \langle L_i, L_j \mathbb{Q}^\top \rangle \hat{\mathbf{E}}_j + \langle L_i, L_j \mathbb{B} \rangle \gamma_j + \langle L_i, L_j \mathbb{R} \rangle \varepsilon_j, \qquad (27)$$

$$\Sigma_i = \langle L_i, \sigma \rangle = \langle L_i, L_j \mathbb{F}^\top \rangle \hat{\mathbf{E}}_j + \langle L_i, L_j \mathbb{R}^\top \rangle \gamma_j + \langle L_i, L_j \mathbb{C} \rangle \varepsilon_j.$$

These can be written as

$$\begin{Bmatrix} \mathbf{N}_i \\ \mathbf{T}_i \\ \Sigma_i \end{Bmatrix} = \begin{pmatrix} \mathbb{A}_{ij} & \mathbb{Q}_{ij} & \mathbb{F}_{ij} \\ \mathbb{Q}_{ij}^\top & \mathbb{B}_{ij} & \mathbb{R}_{ij} \\ \mathbb{F}_{ij}^\top & \mathbb{R}_{ij}^\top & \mathbb{C}_{ij} \end{pmatrix} \begin{Bmatrix} \hat{\mathbf{E}}_j \\ \gamma_j \\ \varepsilon_j \end{Bmatrix}, \qquad (28)$$

where

$$\mathbb{A}_{ij} = \langle L_i, L_j \mathbb{A} \rangle, \qquad \mathbb{Q}_{ij} = \langle L_i, L_j \mathbb{Q} \rangle, \qquad \mathbb{F}_{ij} = \langle L_i, L_j \mathbb{F} \rangle,$$

$$\mathbb{B}_{ij} = \langle L_i, L_j \mathbb{B} \rangle, \qquad \mathbb{R}_{ij} = \langle L_i, L_j \mathbb{R} \rangle, \qquad \mathbb{C}_{ij} = \langle L_i, L_j \mathbb{C} \rangle. \qquad (29)$$

When the material properties do not vary in the thickness direction, $\mathbb{A}_{ij} = \mathbb{A}\delta_{ij}$, etc. and the stress fields of order i are independent of the deformation fields of order $j \neq i$; on the contrary, when using the mixed constitutive relations (23), this does not hold true, since they involve the non-diagonal matrix P_{ij}. Thus mixed relations (23) lead to a more coupled systems of equations but, as we will see, give better results.

In the expansions of all six components of the stress tensor in the z direction, terms upto z^K are kept in this compatible plate theory in contrast to expansions (18) for stresses wherein the transverse shear and the transverse normal stresses have terms up to z^{K+2}. Also, constitutive relations (28) of the higher order compatible plate theory do not necessarily satisfy boundary conditions on the top and the bottom surfaces of the plate but constitutive relations (18) of the higher order plate theory derived from the mixed variational principle do.

4. CONSTITUTIVE RELATIONS CORRESPONDING TO DIFFERENT MATERIAL SYMMETRIES

Whereas constitutive relations (28) of the compatible plate theory involve elasticities of the material, constitutive relations (23) are in terms of material compliances. For a non-homogeneous and anisotropic plate, the matrix of elasticities can be inverted only numerically to obtain the compliance matrix. However, for a homogeneous orthotropic plate with one plane of symmetry coincident with its midsurface, the matrix of elasticities can be inverted analytically. This inversion becomes simpler as the material symmetry increases. For example, for a homogeneous transversely isotropic plate with the unit vector $\mathbf{e}$ as the axis of transverse isotropy, the matrices $\mathbb{H}$, $\mathbb{M}$, $\mathbb{N}$, etc. in constitutive relation (4) are

$$\mathbb{H} = \begin{bmatrix} 2\alpha_1 + \alpha_2 & \alpha_2 & 0 \\ \alpha_2 & 2\alpha_1 + \alpha_2 & 0 \\ 0 & 0 & 2\alpha_1 \end{bmatrix}, \qquad (30)$$

$$\mathbb{M} = \mathbf{0}, \qquad \mathbb{N} = \alpha_4 \tilde{\mathbf{I}}, \qquad \mathbb{G} = (\alpha_3/2)\hat{\mathbf{I}}, \qquad \mathbb{L} = \mathbf{0}, \qquad \mathbb{E} = \alpha_5,$$

where α_1, α_2, α_3, α_4 and α_5 are material parameters, $\tilde{\mathbf{I}} = \{1, 1, 0\}^\top$ and $\hat{\mathbf{I}}$ is the 2×2 identity matrix.

Similarly the matrices appearing in constitutive relation (26) have the representations

$$\mathbb{A} = \begin{bmatrix} 2\gamma_1 + \gamma_2 & \gamma_2 & 0 \\ \gamma_2 & 2\gamma_1 + \gamma_2 & 0 \\ 0 & 0 & 2\gamma_1 \end{bmatrix}, \tag{31}$$

$$\mathbb{Q} = \mathbf{0}, \qquad \mathbb{F} = \gamma_4 \tilde{\mathbf{I}}, \qquad \mathbb{B} = (\gamma_3/2)\hat{\mathbf{I}}, \qquad \mathbb{R} = \mathbf{0}, \qquad \mathbb{C} = \gamma_5,$$

where $\gamma_1, \gamma_2, \gamma_3, \gamma_4$ and γ_5 are material parameters. In terms of the in-plane and transverse Young's moduli (E and E_t), the in-plane and transverse Poisson ratios (v and v_t) and the transverse shear modulus (G_t), we have

$$\alpha_1 = \frac{1+v}{2E}, \quad \alpha_2 = -\frac{v}{E}, \quad \alpha_3 = \frac{1}{G_t}, \quad \alpha_4 = -\frac{v_t}{E}, \quad \alpha_5 = \frac{1}{E_t},$$

$$\gamma_1 = \frac{E}{2(1+v)}, \quad \gamma_2 = \frac{E(v\,\xi_t + v_t^2)}{\xi_t - 2\,v_t^2 - v^2\,\xi_t - 2\,v\,v_t^2}, \quad \gamma_3 = 4G_t, \tag{32}$$

$$\gamma_4 = -\frac{v_t E}{v\xi_t - \xi_t + 2\,v_t^2}, \quad \gamma_5 = \frac{(v-1)E}{v\xi_t - \xi_t + 2v_t^2}, \quad \xi_t = \frac{E}{E_t}, \quad \eta_t = \frac{E}{G_t}.$$

For an isotropic homogeneous plate, relations (32) simplify to

$$4\alpha_1 = \alpha_3 = \frac{1+v}{2E}, \quad \alpha_2 = \alpha_4 = -\frac{v}{E}, \quad \alpha_5 = \frac{1}{E}, \quad \xi_t = 1, \quad \eta_t = 2(1+v),$$

$$\tag{33}$$

$$4\gamma_1 = \gamma_3 = \frac{2E}{(1+v)}, \quad \gamma_2 = \gamma_4 = -\frac{vE}{v-1+2v^2}, \quad \gamma_5 = \frac{(v-1)E}{v-1+2v^2}.$$

Constitutive relations (23) for a transversely isotropic plate with **e** as the axis of transverse isotropy and the top and the bottom surfaces traction free can be written as

$$\hat{\mathbf{E}}_i = 2\alpha_1 \mathbf{N}_i + (\alpha_2(\operatorname{tr} \mathbf{N}_i) + \alpha_4 \Sigma_i)\hat{\mathbf{I}},$$

$$\varepsilon_i = \alpha_4 \operatorname{tr} \mathbf{N}_i + \alpha_5 P_{ij} \Sigma_j, \quad 2\gamma_i = \alpha_3 P_{ij} \mathbf{T}_j; \tag{34}$$

and these equations can be inverted to get

$$\mathbf{N}_i = 2\beta_{1ij}\hat{\mathbf{E}}_j + (\beta_{2ij} \operatorname{tr} \hat{\mathbf{E}}_j + \beta_{4ij} \varepsilon_j)\hat{\mathbf{I}},$$

$$\Sigma_i = \beta_{4ij} \operatorname{tr} \hat{\mathbf{E}}_j + \beta_{5ij} \varepsilon_j, \quad \mathbf{T}_i = 2\beta_{3ij}\gamma_j. \tag{35}$$

Here $\operatorname{tr} \mathbf{N}_i$ equals the sum of the diagonal terms of the matrix $\mathbf{N}_i$. In general, explicit expressions for the coefficients β can be given only in some special cases (depending on the order of the theory). Also, since the matrix P_{ij} is not diagonal and depends on the order of the theory, expressions for all of the parameters β cannot be computed analytically for an arbitrary order K of the theory. However, we can show that

$$\beta_{1ij} = \frac{1}{4\,\alpha_1}\,\delta_{ij} =: \beta_1\,\delta_{ij}, \quad \beta_{3ij} = \frac{1}{\alpha_3}\,P_{ij}^{-1} =: \beta_3\,P_{ij}^{-1}, \tag{36}$$

and that for $a = 1, 2, 3, 4, 5$, $\beta_{aij} = 0$ when $i + j$ is odd. We will analyze the consequences of this last property in the following section. Because of the presence of P_{ij} in equations $(34)_2$ and $(34)_3$, the transverse shear strains and the transverse normal strain at the ith order may depend upon the transverse shear force and the transverse normal force of all orders up to and including the ith order.

5. PLANE WAVE SOLUTIONS IN A TRANSVERSELY ISOTROPIC PLATE

Ericksen [15] has studied plane infinitesimal waves in a homogeneous elastic plate by using the Cosserat theory of plates [10], and discussed conditions under which frequencies corresponding to real wave vectors must be real. Yang *et al.* [16] have used the first order shear deformation theory to study wave propagation in an infinite two-layer isotropic plate undergoing plane strain deformations.

We seek solutions of equations (15) and (23) in the form of travelling plane waves, i.e.,

$$\begin{Bmatrix} \mathbf{v}_i(\mathbf{r}, t) \\ w_i(\mathbf{r}, t) \end{Bmatrix} = \mathrm{Re}\left(\begin{Bmatrix} \mathbf{V}_i \\ W_i \end{Bmatrix} \exp\left[I(\omega t - \mathbf{k} \cdot \mathbf{r}) \right] \right), \tag{37}$$

where $I = \sqrt{-1}$, ω is the circular frequency, $\mathbf{V}_i$ and W_i are constants, $\mathbf{k} = \kappa \mathbf{v}$, $\mathbf{v} = \cos\theta\, \mathbf{e}_1 + \sin\theta\, \mathbf{e}_2$ is the direction of propagation of the plane wave, $\mathbf{e}_1$ and $\mathbf{e}_2$ are orthonormal vectors in the plane $\mathscr{S}$ and $\mathrm{Re}(\cdot)$ denotes the real part of $(\cdot)$. Using the Euler relation we obtain

$$\mathrm{Re}[(a + I b)\exp(c + I d)] = \exp(c)\left[a\cos(d) - b\sin(d) \right], \tag{38}$$

where a, b, c and d are real numbers. Thus, in our representation, the real and the imaginary parts of κ equal, respectively, the inverse of the wavelength and the inverse of the length of decay; the real and the imaginary parts of the associated eigenvectors are the sine and the cosine components of the wave form. Moreover, the ratio $\omega/\mathrm{Re}(\kappa)$ is the phase speed. In the following we omit writing $\mathrm{Re}(\cdot)$ on the right-hand side.

Substitution for $\mathbf{v}_i$ and w_i from equation (37) into equation (9) yields

$$\hat{\mathbf{E}}_j = - I\kappa\, \mathrm{sym}\, (\mathbf{V}_j \otimes \mathbf{v}) \exp[I(\omega t - \mathbf{k} \cdot \mathbf{r})],$$

$$\boldsymbol{\gamma}_j = \tfrac{1}{2}(D_{kj}\mathbf{V}_k - I\kappa\, W_j\mathbf{v}) \exp[I(\omega t - \mathbf{k} \cdot \mathbf{r})], \tag{39}$$

$$\varepsilon_j = D_{kj}\, W_k \exp[I(\omega t - \mathbf{k} \cdot \mathbf{r})],$$

while, using constitutive relations (35) for a transversely isotropic material, the stress resultant fields become

$$\mathbf{N}_i = \left[- 2\, I\, \kappa \beta_{1ij}\, \mathrm{sym}\, (\mathbf{V}_j \otimes \mathbf{v}) + (\beta_{4ij} D_{kj} W_k - I\, \kappa\, \beta_{2ij}\mathbf{V}_j \cdot \mathbf{v})\hat{\mathbf{I}} \right] \exp[I(\omega t - \mathbf{k} \cdot \mathbf{r})],$$

$$\Sigma_i = \left[- I\, \kappa\beta_{4ij}(\mathbf{V}_j \cdot \mathbf{v}) + \beta_{5ij} D_{kj} W_k \right] \exp[I(\omega t - \mathbf{k} \cdot \mathbf{r})],$$

$$\mathbf{T}_i = \beta_{3ij}(D_{kj}\mathbf{V}_k - I\, \kappa\, W_j\mathbf{v}) \exp[I(\omega t - \mathbf{k} \cdot \mathbf{r})]. \tag{40}$$

Substituting for $\mathbf{N}_i$, Σ_i and $\mathbf{T}_i$ from equation (40) into balance laws (15), we get the following set of simultaneous linear equations in $\mathbf{V}_i$ and W_k:

$$[\kappa^2 (\beta_{1ij}(\hat{\mathbf{I}} + \mathbf{v} \otimes \mathbf{v}) + \beta_{2ij} \mathbf{v} \otimes \mathbf{v}) - \rho \, \omega^2 \, \delta_{ij} \hat{\mathbf{I}}] \, \mathbf{V}_j$$

$$+ D_{ij} \beta_{3jh} D_{kh} \mathbf{V}_k + I \kappa (\beta_{4ij} D_{kj} - D_{ij} \beta_{3jk}) W_k \mathbf{v} = \mathbf{0},$$

$$(\beta_{3ij} \kappa^2 - \rho \omega^2 \delta_{ij}) W_j + D_{ij} \beta_{5jh} D_{kh} W_k + I \kappa (\beta_{3ij} D_{kj} - D_{ij} \beta_{4jk})(\mathbf{V}_k \cdot \mathbf{v}) = 0,$$

$$i, j, k, h = 0, 1, \dots, K. \tag{41}$$

The requirement that system of equations (41) have a non-trivial solution leads to the dispersion relation

$$\kappa_n = F_n(\omega), \qquad n = 1, 2, \dots, 6(K + 1), \tag{42}$$

where for each frequency ω, the real part of $F_n(\omega)$ represents the inverse of the associated nth wavelength, while the imaginary part represents the inverse of its length of decay. For each set $\{\omega, F_n(\omega)\}$, the non-trivial solution of equations (41) gives the associated wave form $(\mathbf{V}_0, W_0, \mathbf{V}_1, W_1, \dots, \mathbf{V}_K, W_K)$.

5.1. SHEAR, MEMBRANAL AND FLEXURAL PROBLEMS

In this section, we adopt the classical partition of wave-propagation problems into simplest cases appropriate for plate theories of arbitrary order K.

Definition. An $n \times n$ matrix $\mathbf{M}$ is said to be *chessboard*-0 (*chessboard*-1) if its components satisfy the relation $M_{ij} = 0$ when $i + j$ is odd (even). We denote by C^0 (C^1) the vector space of chessboard-0 (chessboard-1) matrices. Thus, for instance, the even components of the vector $(\mathbf{M} \mathbf{v})$ do not depend on the odd components of the vector $\mathbf{v}$ if $\mathbf{M} \in \mathsf{C}^0$.

Proposition. *The following statements are true*:

$$\mathbf{M} \in \mathsf{C}^0, \text{ and } \mathbf{M}^{-1} \text{ exists} \ \Rightarrow \ \mathbf{M}^{-1} \in \mathsf{C}^0,$$

$$\mathbf{M}, \mathbf{N} \in \mathsf{C}^0, \text{ or } \mathbf{M}, \mathbf{N} \in \mathsf{C}^1 \ \Rightarrow \ (\mathbf{M} \circ \mathbf{N}) \in \mathsf{C}^0, \tag{43}$$

$$\mathbf{M} \in \mathsf{C}^0, \mathbf{N} \in \mathsf{C}^0 \ \Rightarrow \ (\mathbf{M} \circ \mathbf{N}) \in \mathsf{C}^1,$$

where $\mathbf{M} \circ \mathbf{N}$ *denotes the multiplication of matrices* $\mathbf{M}$ *and* $\mathbf{N}$.

We are now able to prove the

Theorem. *The* $3(K + 1)$ *scalar equations* (41) *can be partitioned into the direct sum of four different uncoupled problems of sizes* $(K + 1)/2, (K + 1)/2, K + 1$ *and* $K + 1$.

Proof. Let U_i and V_i represent, respectively, components of the ith displacement parallel and normal to the direction of wave propagation. That is,

$$V_i = U_i \mathbf{v} + V_i \tau, \quad \tau \cdot \mathbf{v} = 0, \quad \tau \cdot \tau = 1.$$

Then equations (41) reduce to

$$(\kappa^2\beta_1 - \rho\omega^2)\,V_i + \beta_3\,D_{ij}\,P_{jh}^{-1}\,D_{kh}\,V_k = 0,$$

$$[\kappa^2(\beta_1\,\delta_{ij} + \beta_{2ij}) - \rho\omega^2\delta_{ij}]\,U_j + \beta_3 D_{ij}P_{jh}^{-1}D_{kh}U_k + I\kappa\,(\beta_{4ij}D_{kj} - \beta_3 D_{ij}P_{jk}^{-1})\,W_k = 0,$$

$$(\kappa^2\beta_3\,P_{ij}^{-1} - \rho\omega^2\,\delta_{ij})\,W_j + D_{ij}\beta_{5jh}\,D_{kh}\,W_k + I\kappa\,(\beta_3\,P_{ij}^{-1}\,D_{kj} - D_{ij}\,\beta_{4jk})\,U_k = 0. \qquad (44)$$

Since the polynomials L_i and $\tilde{L}_i$ are, by construction, alternatively even and odd on the interval $[-h, h]$, we find that $D_{ij} \in \mathsf{C}^1$ and $P_{ij} \in \mathsf{C}^0$. Moreover, we have $\delta_{ij} \in \mathsf{C}^0$ and $\beta_{aij} \in \mathsf{C}^0$ for $a = 1, 2, 3, 4$ and 5. By means of the above proposition, $D_{ij}P_{jh}^{-1}D_{kh} \in \mathsf{C}^0$, but both $\beta_{aij}D_{kj}$ and $P_{ij}^{-1}D_{jk}$ belong to C^1.

It follows that the following partition of the eigenvectors

$$\{U_0, V_0, W_0, \dots, U_i, V_i, W_i, \dots, \} = \{V_0, V_2, V_4, \dots\}$$

$$\cup \{V_1, V_3, V_5, \dots\}$$

$$\cup \{U_0, W_1, U_2, W_3, U_4, W_5, \dots\}$$

$$\cup \{W_0, U_1, W_2, U_3, W_4, U_5, \dots\} \qquad (45)$$

induces a partition of equations (44) into the four respective uncoupled problems: transverse symmetric (T0), transverse skew-symmetric (T1), longitudinal membranal (LM) and longitudinal flexural (LF) waves. ∎

The adjectives "transverse" and "longitudinal" imply that in the first case the displacement is purely orthogonal to the direction of propagation while in the second case there are also components of the displacement parallel to the propagation direction.

Finally, we remark that equations (44) and, as a consequence, their decomposition still holds for a compatible higher order plate theory but is not valid when either (a) the material anisotropy is such that tensors $\mathbb{M}$ and $\mathbb{L}$ (or $\mathbb{Q}$ and $\mathbb{R}$) are not zeroes (this will be the case when the axis of transverse isotropy is not along the normal to the midsurface of the plate); or (b) the material, although isotropic, has properties varying in the thickness direction, e.g., a plate made of an inhomogeneous material. In these cases the constitutive relations (44) could be inverted numerically, but no *a priori* prediction of the decomposition of the wave forms is possible.

In terms of the non-dimensional variables denoted below by a superimposed tilde, equations (44) become

$$(\tilde{\kappa}^2 - \varpi^2)\,\tilde{V}_i + \tilde{\beta}_3\,\tilde{D}_{ij}\,P_{jh}^{-1}\,\tilde{D}_{kh}\,\tilde{V}_k = 0,$$

$$[\tilde{\kappa}^2(\delta_{ij} + \tilde{\beta}_{2ij}) - \varpi^2\,\delta_{ij}]\,\tilde{U}_j + \tilde{\beta}_3\,\tilde{D}_{ij}\,P_{jh}^{-1}\,\tilde{D}_{kh}\,\tilde{U}_k + I\,\tilde{\kappa}(\tilde{\beta}_{4ij}\,\tilde{D}_{kj} - \tilde{\beta}_3\,P_{ij}^{-1}\,\tilde{D}_{jk})\,\tilde{W}_k = 0,$$

$$(\tilde{\kappa}^2\,\tilde{\beta}_3\,P_{ij}^{-1} - \varpi^2\,\delta_{ij})\,\tilde{W}_j + \tilde{D}_{ij}\,\tilde{\beta}_{5jh}\,\tilde{D}_{kh}\,\tilde{W}_k + I\,\tilde{\kappa}(\tilde{\beta}_3\,P_{ij}^{-1}\,\tilde{D}_{kj} - \tilde{\beta}_{4ij}\,\tilde{D}_{jk})\,\tilde{U}_k = 0, \qquad (46)$$

where

$$\tilde{\kappa} = h\,\kappa, \qquad \tilde{\beta}_{aij} = \beta_{aij}/\beta_1, \qquad \tilde{\mathbf{v}}_k = \mathbf{v}_k/h, \qquad \tilde{D}_{ij} = h\,D_{ij}, \qquad \varpi^2 = h^2\,\rho\omega^2/\beta_1. \qquad (47)$$

Since the thickness of the plate appears in the definition of the dimensionless frequency ϖ, a thin plate at high frequencies behaves similar to a thick plate at low frequencies.
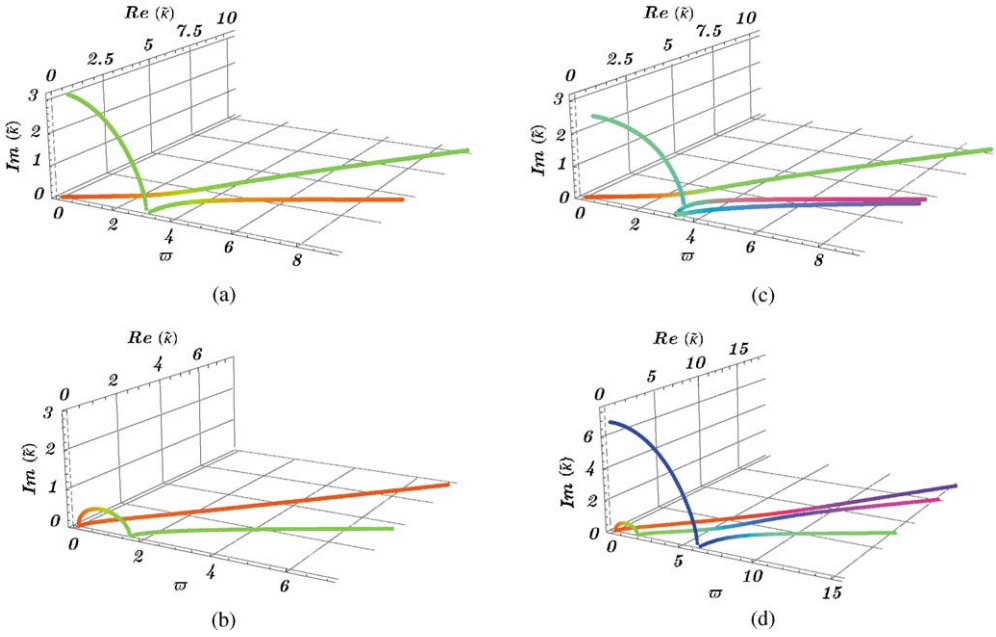
Figure 3. Solutions of dispersion relation (42). (a) Longitudinal membranal (LM) waves for $K = 1$; components U_0 (red) and W_1 (green). (b) Longitudinal flexural (LF) waves for $K = 1$; components W_0 (red) and U_1 (green). (c) LM waves for $K = 2$; components U_0 (red), W_1 (green) and U_2 (blue). (d) LF waves for $K = 2$; components W_0 (red), U_1 (green) and W_2 (blue).

5.2 COMPLEX ROOTS OF THE DISPERSION RELATION AND INTERACTIONS

A complete description of the solutions of dispersion formula (42) is shown in Figures 3–5 for a homogeneous isotropic material with the Poisson ratio $v = 0.33$. In Figure 3, the colors indicate the displacement components of the associated eigenvectors.

In Figure 3(a), the green branch is for W_1 and means a wave of uniform stretching of the thickness, while the red branch is associated with U_0 and signifies a pure longitudinal wave with constant displacement through the thickness; these kind of waves, involving in-plane deformations and thickness distension, have been analyzed also by Di Carlo *et al.* [9]. After a certain value of the non dimensional frequency ϖ the W_1 waves do not decay anymore. Moreover, a veering phenomenon between the red and the green branches occurs at $\varpi \simeq 3$; in the region of distortion there is neither a purely red nor a purely green wave. In other words, in that region the longitudinal waves necessarily involve a change in thickness and *vice versa*. Finally, for high values of ϖ all of the branches tend to become straight lines (non-dispersive waves[†]). Figure 3(c) depicts a refinement of these phenomena through the introduction of U_2 (blue color); this describes a longitudinal (in the direction of **v**) displacement field parabolic in z, whose average value over the thickness and the first moment vanish, as shown in Figure 1. As Figure 3(c) shows, for high frequencies this field is intrinsically coupled with the W_1 waves.

[†]A wave is said to be non-dispersive if the group velocity equals the phase velocity, i.e.,

$$\frac{\partial \varpi}{\partial \mathrm{Re}(\tilde{\kappa})} = \frac{\varpi}{\mathrm{Re}(\tilde{\kappa})};$$

thus if the relation between $\mathrm{Re}(\tilde{\kappa})$ and ϖ is linear, then the wave is non-dispersive.

Figure 4. Solutions of dispersion relation (42) for $K = 3$. The imaginary part of $\tilde{\kappa}$ is represented by gray curves, the real part by black curves.

Results for the longitudinal flexural waves are shown in Figures 3(b) and 3(d). For $K = 1$, they involve the usual shear waves associated with W_0 (red branches) and the conventional rotation waves associated with U_1 (green branches). For low dimensionless frequencies they are coupled together and give rise to the conventional bending waves; this coupling vanishes after a certain value of ϖ. Note that the shear-wave branch is non-dispersive. Finally, for $K = 2$ the descriptor W_2 (blue color) is also involved; it does not change the aforementioned behavior for low values of ϖ but interacts through a double veering with both the red and the green branches for $\varpi \in (5, 10)$ (cf., Figure 3(d)).

For $K > 2$ there is no way to associate an independent color to each component of the eigenvector, so the waves are represented as follows. Figures 4 and 5, respectively, represent the wave solutions for $K = 3$ and 4; the gray color indicates the imaginary part of $\tilde{\kappa}$ while the dark curves signify the real part.

As expected, with an increase in the order K of the plate theory, we get new wave solutions that describe the propagation of the high order displacement fields. For low
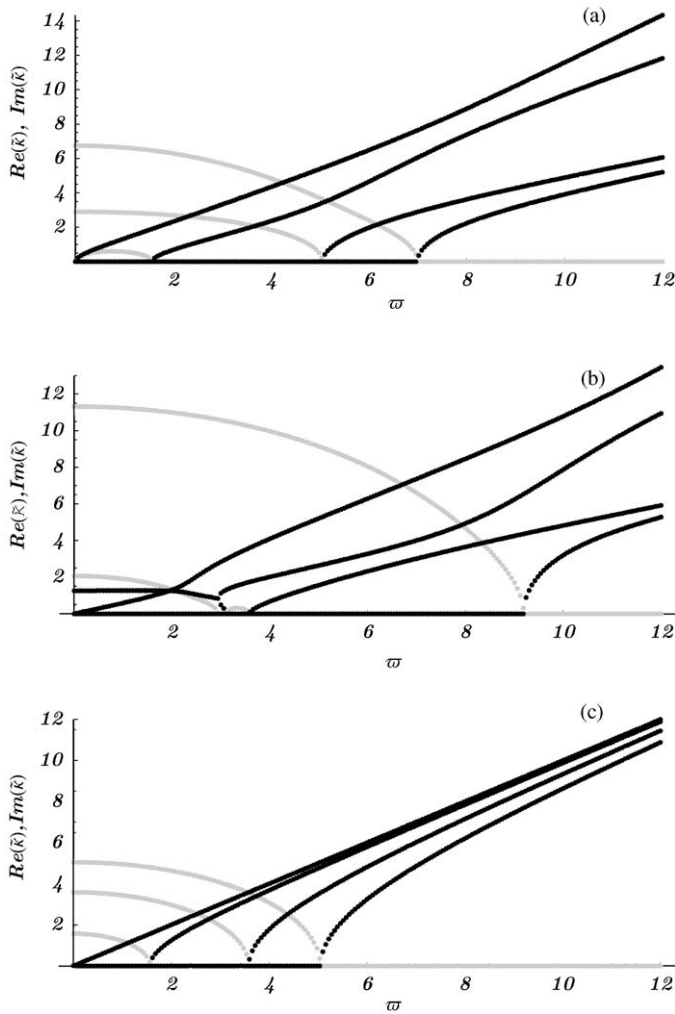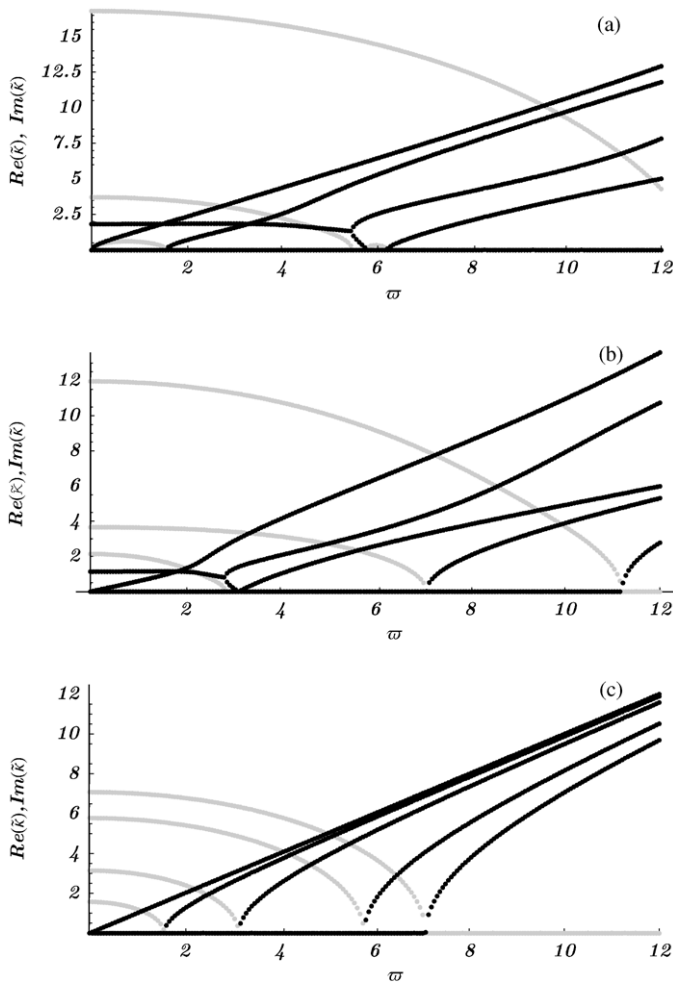
Figure 5. Solutions of dispersion relation (42) for $K = 4$. The imaginary part of $\tilde{\kappa}$ is represented by gray curves, the real part by black curves. (a) LF, (b) LM, (c) T0–T1.

dimensionless frequencies these higher order solutions show relevant imaginary parts of the wavelength or, in other words, small lengths of decay. However, there are some critical values of frequencies beyond which all waves have vanishing damping ratios and exhibit non-dispersive behaviors. Typically, the higher is the polynomial order of the displacement descriptor introduced, the smaller is the associated length of decay, i.e., the size of the induced boundary layer.

The following questions arise: do the displacement fields of order K always decay faster than the displacement fields of order $(K - 1)$? Which components of the displacement decay the most? How do the material properties influence this ordering?

In the case of T0–T1 waves in a transversely isotropic plate, for every order K, the intercepts of the gray lines with the axes $\varpi = 0$ and $\mathrm{Im}(\tilde{\kappa}) = 0$ are proportional to $\sqrt{(1 + v)\, G_t/E}$. In other words, the lengths of decay under static conditions and the critical frequencies—after which the waves do not decay anymore—are proportional to the ratio between the transverse and the in-plane shear moduli. The ordering of the T0–T1 displacement descriptors V_i is then trivial; refer to Figures 4 and 5.

For the LM and the LF waves the situation is more complicated, and depends on the order of the theory. An analytical solution cannot be found for an arbitrary order of the plate theory. For $K = 1$ and the LM waves (or for $K = 2$ and the LF waves) the intercept of the green (blue) curve with the plane $\varpi = 0$ in Figures 3(a) and 3(d) is proportional to $\sqrt{\eta_t/4\,(\xi_t - v_t^2)}$; while the critical frequency, the intercept of the same curve with the plane $\mathrm{Im}(\kappa) = 0$, is proportional to $\sqrt{2\,(1 - v^2)/\xi_t\,(1 - v) - 2\,v_t^2}$. Thus, in a material very soft in the thickness direction and very stiff in the in-plane directions, the critical frequency, after which the W_1 wave (or the W_2 wave) has vanishing damping, can be small; thus a plate model without the descriptors W_1 (W_2) can have a small range of predictability. Anyway, the ordering of the LM and LF displacement descriptors U_i and W_i, in terms of decaying properties is not obvious and will be analyzed in detail in the following section.

5.3. LENGTHS OF DECAY

We now analyze in more detail the wave solutions under quasistatic conditions, i.e., $\varpi \simeq 0$, and elucidate upon the relative importance of various displacement field descriptors (namely the fields U_i, V_i, W_i), i.e., which ones decay the most and at what distances from a unitary source. It will enable one to choose a plate theory of order K that is not complete, i.e., in which some components of the displacement fields are neglected due to their decay properties: two different examples, considering both an isotropic and a transversely isotropic material, are presented in order to elucidate this concept.

Recall that, the amplitude of the plane wave associated with $\kappa \in \mathbb{C}$ is reduced by the factor $\exp(-\delta)$ at a distance $d = \delta h/|\mathrm{Im}(\tilde{\kappa})|$ where $2h$ equals the plate thickness. For an isotropic material with the Poisson ratio $v = 0.33$, Table 1 shows for the four different waves the

TABLE 1

Lengths of 95% decay in the wave amplitude and the associated eigenvectors for the four different waves in an isotropic homogeneous plate

95% decay	$1 \to 0.8$	$0.8 \to 0.6$	$0.6 \to 0.4$	$0.4 \to 0.2$
LF waves				
∞	W_0			
$0.800h$		W_2	U_3	W_4, U_5
$0.562h$		U_5	U_7	W_4, W_6
$0.381h$			W_4, U_5, W_6	W_2, U_7
$0.083h$		W_6	W_4	W_2
LM waves				
$1.424h$		W_1	U_2	W_3
$0.567h$			U_4, W_3, W_5	W_1, U_6
$0.330h$			U_6, W_7, W_5, W_3	W_1
$0.074h$		W_7	W_5	W_1, W_3
T0–T1 waves				
∞	V_0			
$1.910h$	V_1			
$0.955h$	V_2			V_4
$0.637h$	V_3		V_5	
$0.467h$	V_4		V_6	V_2
$0.376h$		V_5, V_7		V_3
$0.209h$	V_6		V_4	
$0.202h$		V_7	V_5	V_3

TABLE 2

Lengths of 95% decay in the wave amplitude and the associated eigenvectors for the four different waves in a transversely isotropic homogeneous plate

95% decay	$1 \to 0.8$	$0.8 \to 0.6$	$0.6 \to 0.4$	$0.4 \to 0.2$
LF waves				
∞	W_0			
$3.480h$	W_0		U_3	U_5
$2.021h$		W_0	U_5, U_7	U_3
$1.078h$		W_0	W_2, U_7	U_5
$0.608h$	W_2			W_4
$0.293h$	W_4		W_6	W_2
$0.084h$	W_6		W_4	W_2
LM waves				
$4.925h$	U_2			W_1, U_4
$2.393h$		U_4	W_1, U_6	U_2
$1.168h$	W_1			
$0.400h$	W_3		W_5	
$0.239h$		W_5, W_7		W_3
$0.077h$		W_7	W_5	W_3
T0–T1 waves				
∞	V_0			
$5.971h$	V_1			
$2.986h$	V_2			V_4
$1.990h$	V_3		V_5	
$1.462h$	V_4		V_6	V_2
$1.176h$		V_5, V_7		V_3
$0.654h$	V_6		V_4	
$0.633h$		V_7	V_5	V_3

lengths of a 95% decay and the associated eigenvectors. The components of eigenvectors normalized to have unit Euclidean norm are divided into four columns of relative importance. Because of this normalization, a displacement component can have a maximum value of one. For each wave type, the amplitudes of the displacement vector are divided into four groups with magnitudes in the range 0·2–0·4, 0·4–0·6, 0·6–0·8 and 0·8–1·0; those with amplitude less than 0·2 are ignored. For instance, the second row of Table 1 implies that for the LF waves the eigenvector, constituted by the contribution of W_2 between 0·8 and 0·6, U_3 between 0·6 and 0·4, and W_4 and U_5 between 0·4 and 0·2, decays after a distance of 0·8h from the unitary source to 5% of its initial amplitude. Since the initial amplitude (i.e., the square root of the sum of squares of displacement components) of the wave equals 1, after the 95% decay it is reduced to 0·05. Even though we have not listed the magnitude of each component, their relative magnitudes remain unaltered because they are the components of an eigenvector.

Table 2 shows analogous results in terms of 95%-decay lengths for a transversely isotropic material with $v = 0.33$, $v_t = 0.33$, $\xi_t = 10$, $\eta_t = 26$. Again the components of eigenvectors, normalized to have unit Euclidean norm, are divided into four columns of relative importance.

From the aforestated results, it is evident that, while the hierarchy of the T0–T1 waves is straightforward, that of LM and LF waves containing displacements U_i and W_i is more involved. Depending on the material of the plate and the problem being examined, a higher

order descriptor field can decay less than a lower order descriptor field. For example in Table 2 for the LF waves, the contributions of U_5 and U_7 to the eigenvectors are between 0·4 and 0.6 while that of U_3 is between 0·2 and 0·4. Similarly, from Table 2, one can conclude that for studying deformations associated with the LM waves, one can use an incomplete theory with kinematic variables U_0, U_2, W_1, U_4 and U_6, and neglect W_3 and W_5 since the waves involving W_3 and W_5 have a much smaller length of decay.

6. MODAL ANALYSIS FOR A SIMPLY SUPPORTED PLATE

In a rectangular plate of sides a and b let $\mathbf{e}_1$, $\mathbf{e}_2$ be the two orthonormal vectors parallel to the sides; moreover let $\mathbf{r} = x\,\mathbf{e}_1 + y\,\mathbf{e}_2$. At the simply supported edges we apply the boundary conditions

$$\bar{w} = \bar{\mathbf{v}}_2 = \mathbf{t}_1 = 0, \qquad \text{on } x = 0, a,$$
$$\bar{w} = \bar{\mathbf{v}}_1 = \mathbf{t}_2 = 0, \qquad \text{on } y = 0, b,$$

(48)

or in terms of the plate theory

$$w_i = v_{2i} = N_{11i} = 0, \qquad \text{on } x = 0, a,$$
$$w_i = v_{1i} = N_{22i} = 0, \quad \text{on } y = 0, b, \quad i = 0, 1, 2, \dots, K.$$

(49)

The boundary conditions (48) are the same as those presumed by Srinivas and Rao [11]. These authors employed the three-dimensional elasticity equations to study free vibrations of a simply supported rectangular plate. For studying free vibrations of the plate, we assume that there are neither body forces nor surface tractions acting on the top and the bottom surfaces of the plate.

We seek solutions of balance equations (15), constitutive relations (23) and boundary conditions (49) in the form

$$v_{1i} = U_{imn}\, e^{I\omega t} \cos(m\,\pi\,x/a) \sin(n\,\pi\,y/b),$$
$$v_{2i} = V_{imn}\, e^{I\omega t} \sin(m\,\pi\,x/a) \cos(n\,\pi\,y/b), \qquad m,\, n = 1, 2, \dots M.$$

(50)

$$w_i = W_{imn}\, e^{I\omega t} \sin(m\,\pi\,x/a) \sin(n\,\pi\,y/b),$$

For each given pair (m, n) we obtain a linear eigenvalue problem for the determination of the frequency ω and the corresponding mode vector $\{, \dots, U_{imn}, V_{imn}, W_{imn}, \dots\}$. The procedure is standard and we do not provide, for sake of brevity, the final form of the eigenvalue problem.

The present results are compared with those of Srinivas and Rao; to this aim the plate is assumed to be made of an Aragonite crystal, whose material parameters are listed in reference [11], an homogeneous and orthotropic material with one plane of symmetry coincident with the midsurface of the plate.

Following the reasoning similar to that used to prove the theorem of section 4.1, this system is decomposed into two sets of uncoupled equations, namely a membranal problem —with deformations symmetric about the midplane and labelled by Srinivas and Rao with the letter "S"—involving the variables $\{U_{0mn}, V_{0mn}, W_{1mn}, U_{2mn}, V_{2mn}, W_{3mn}, U_{4mn}, V_{4mn}, W_{5mn}, \dots\}$ and a flexural problem—with deformations antisymmetric about the midplane and labelled by Srinivas and Rao with the letter "A"—involving the variables $\{U_{1mn}, V_{1mn}, W_{0mn}, U_{3mn}, V_{3mn}, W_{2mn}, U_{5mn}, V_{5mn}, W_{4mn}, \dots\}$.

6.1. COMPARISON OF EIGENVALUES

In Table 3, for $2mh/a = 0.5$ and $2nh/b = 0.1, 0.2, \ldots, 0.5$, the first eight dimensionless eigenvalues

$$\lambda := 2\omega h \sqrt{\frac{\rho}{\mathbb{A}_{11}}}, \tag{51}$$

computed for plate theories of different order (i.e., different values of K), are compared with the exact results of Srinivas and Rao [11]. Results for the Kirchhoff plate theory and the Mindlin plate theory are taken from their paper. Symbols 1C, 3C, etc. signify results computed with the first order ($K = 1$) and third order ($K = 3$) plate theories but using compatible constitutive relations (28). Symbols 1M, 3M, etc. denote results obtained with the first and the third order plate theories and constitutive relations (23). All results are compared in terms of percent errors, i.e., $100(\lambda_{ex} - \lambda_{appr})/\lambda_{ex}$.

We note that the Kirchhoff plate theory and the Mindlin plate theory are incapable of predicting any of the S-modes of vibration which involve in-plane deformations of the plate. The order of the plate theory that gives accurate values of frequencies increases with the mode number considered. For example, for modes I-A, I-S, II-A and II-S, the present first order shear and normal deformable plate theory gives frequencies within 0.65% of their exact values. However, for modes III-A and III-S, one needs a third order shear and normal deformable plate theory to compute frequencies within 0.42% of their analytical values. For modes IV-S and V-S, a fifth order shear and normal deformable plate theory is needed to obtain accurate values (within 0.3% of the exact values) of the frequencies, and frequencies computed with the present and hence any third order shear and normal deformable plate theory have errors of about 10%. For $2h/a = 2h/b = 0.1$ and $m, n = 1, 2$ and 3, Chao *et al.* [4] show that their third order shear and normal deformable plate theory (which is identical to the present compatible plate theory with $K = 3$) gives frequencies that agree exactly with the analytical solution of Srinivas and Rao [11]. Kant and Swaminathan [17] have compared the analytical frequencies of Srinivas and Rao [11] with those obtained from five different plate theories, four of which neglect the transverse normal strains and one is essentially identical to that of Chao *et al.* [4] but published prior to Chao *et al.*'s work. However, both Chao *et al.* [4] and Kant and Swaminathan [17] consider only modes of vibration that are antisymmetric about the midplane of the plane. Results presented in Table 3 reveal that the errors in the frequencies of the fourth and the fifth modes of vibrations symmetric about the midplane and computed with the third order shear and normal compatible plate theory are about 10 and 35% respectively. At least a fifth order either compatible or the present shear and normal deformable plate theory is needed to reduce these errors to less than 0.6%. The present shear and normal deformable Kth order plate theory involves $3(K + 1)$ unknowns at each point of the midsurface of the plate. For every fixed value of K, results computed with the mixed constitutive relations (23) yield considerably less error than those computed with the compatible constitutive relations (28); as a matter of fact, only in the former model the boundary conditions on the top and bottom surfaces of the plate exactly are satisfied.

6.2. COMPARISON OF STRESS DISTRIBUTIONS

Recalling that the exact solution is found by the method of separation of variables, the ratios $S_{xx}(\mathbf{r}, z)/S_{xx}(\mathbf{r}, \bar{z})$, $S_{yy}(\mathbf{r}, z)/S_{yy}(\mathbf{r}, \bar{z})$, $\ldots$, $\sigma(\mathbf{r}, z)/\sigma(\mathbf{r}, \bar{z})$, for z and $\bar{z} \in (-h, h)$, are

TABLE 3

For an Aragonite crystal (*orthotropic*) *simply supported rectangular plate, comparison of exact frequencies with those computed from the present higher order plate theory*

			% error							
$2mh/a$	$2nh/b$	Exact value	Kirch.	Mindlin	1C	1M	3C	3M	5C	5M
Mode I-A										
0·5	0·1	0·45265	62·10	− 0·393	9·475	− 0·394	0·062	0·008	0·002	0·000
0·5	0·2	0·48680	63·95	− 0·446	9·453	− 0·445	0·066	0·010	0·006	0·000
0·5	0·3	0·54160	67·02	− 0·523	9·462	− 0·524	0·079	0·014	0·015	0·000
0·5	0·4	0·61465	71·25	− 0·621	9·518	− 0·621	0·101	0·020	0·029	0·000
0·5	0·5	0·70338	76·52	− 1·031	9·615	− 0·726	0·130	0·028	0·045	0·000
Mode I-S										
0·5	0·1	0·81720	—	—	0·030	0·005	0·008	0·000	0·004	0·000
0·5	0·2	0·85223	—	—	0·112	0·021	0·026	0·000	0·014	0·000
0·5	0·3	0·90962	—	—	0·226	0·051	0·048	0·000	0·025	0·000
0·5	0·4	0·98732	—	—	0·351	0·094	0·065	0·000	0·034	0·000
0·5	0·5	1·08240	—	—	0·476	0·149	0·075	0·001	0·038	0·000
Mode II-S										
0·5	0·1	1·5890	—	—	0·011	0·003	0·001	0·000	0·000	0·000
0·5	0·2	1·6425	—	—	0·027	0·008	0·002	0·000	0·001	0·000
0·5	0·3	1·7266	—	—	0·074	0·026	0·005	0·000	0·002	0·000
0·5	0·4	1·8350	—	—	1·087	0·084	0·010	0·001	0·004	0·000
0·5	0·5	1·9596	—	—	6·178	0·277	0·023	0·007	0·005	0·000
Mode II-A										
0·5	0·1	1·8056	—	0·521	16·24	0·519	0·040	0·001	0·001	0·000
0·5	0·2	1·7974	—	0·517	15·32	0·514	0·057	0·004	0·005	0·000
0·5	0·3	1·7999	—	0·533	14·59	0·534	0·086	0·009	0·009	0·000
0·5	0·4	1·8187	—	0·577	12·88	0·575	0·124	0·018	0·013	0·000
0·5	0·5	1·8559	—	0·571	7·116	0·630	0·168	0·028	0·016	0·000

TABLE 3

Continued

|			% error							
$2mh/a$	$2nh/b$	Exact value	Kirch.	Mindlin	1C	1M	3C	3M	5C	5M
Mode III-A										
0·5	0·1	2·0667	—	0·498	10·29	0·499	0·107	0·025	0·000	0·000
0·5	0·2	2·1344	—	0·614	10·86	0·613	0·156	0·039	0·002	0·000
0·5	0·3	2·2288	—	0·767	11·08	0·771	0·234	0·062	0·005	0·000
0·5	0·4	2·3412	—	0·970	16·18	3·532	0·341	0·095	0·008	0·000
0·5	0·5	2·4665	—	1·216	22·85	1·216	0·480	0·141	0·011	0·000
Mode III-S										
0·5	0·1	2·2395	—	—	28·16	5·351	0·891	0·418	0·004	0·002
0·5	0·2	2·2386	—	—	29·13	5·968	0·878	0·403	0·004	0·001
0·5	0·3	2·2380	—	—	30·67	6·957	0·868	0·386	0·004	0·001
0·5	0·4	2·2394	—	—	26·91	5·560	0·868	0·376	0·006	0·000
0·5	0·5	2·2468	—	—	21·99	9·629	0·872	0·371	0·011	0·000
Mode IV-S										
0·5	0·1	3·0334	—	—	—	—	28·80	10·30	0·411	0·195
0·5	0·2	3·0174	—	—	—	—	29·42	10·59	0·405	0·192
0·5	0·3	3·0040	—	—	—	—	29·99	10·84	0·398	0·188
0·5	0·4	3·0000	—	—	—	—	30·29	10·95	0·390	0·183
0·5	0·5	3·0082	—	—	—	—	30·25	10·90	0·381	0·178
Mode V-S										
0·5	0·1	3·3648	—	—	—	—	36·66	13·17	0·464	0·218
0·5	0·2	3·4204	—	—	—	—	35·57	12·75	0·479	0·226
0·5	0·3	3·4991	—	—	—	—	34·27	12·30	0·500	0·237
0·5	0·4	3·5931	—	—	—	—	32·99	11·91	0·529	0·251
0·5	0·5	3·6979	—	—	—	—	31·83	11·60	0·565	0·270
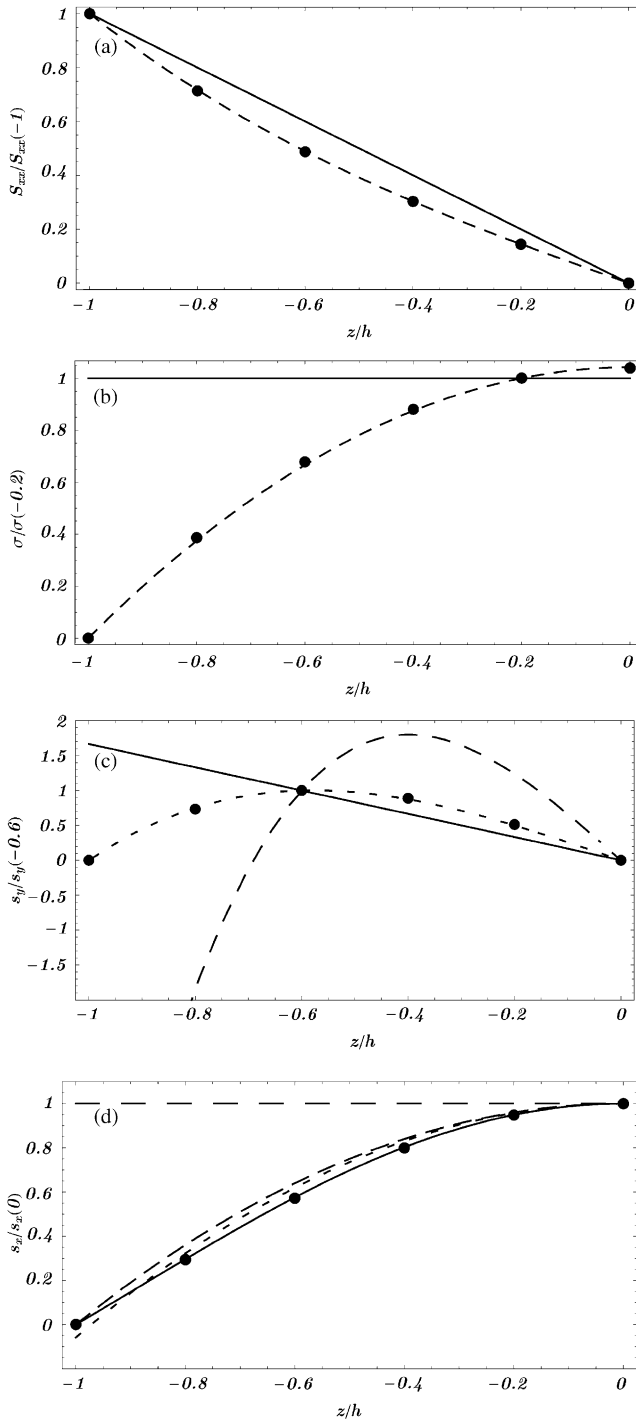
Figure 6. Comparison of through-the-thickness distribution of stresses computed from the present plate theory with the exact solution of Srinivas and Rao which is denoted by filled circles. (a) Mode I-A: (——) 1M, 1C; (---) 3M, 3C. (b) Mode I-S: (——) 1C; (---) 1M, 3C. (c) Mode II-S: (——) 1C; (---) 1M; (– –) 3C. (d) Mode III-A: (——) 3M; (---) 3C; (– –) 1M; (———) 1C.

independent of the values of the in-plane position vector **r**. Thus in Figure 6, for several choices of $\bar{z} \in (-h, h)$ indicated in the axes labels, the ratios of different stress components are plotted as a function of z/h for $mh/a = nh/b = 0.15$ and four modes of vibration. The filled circles denote exact values taken from Table 6 of Srinivas and Rao [11]. The order of the plate theory used is the minimum one that gives a good agreement with the analytical values. It is evident that the third order shear and normal deformable plate theory (3M) not only gives accurate values of the frequencies but also of the through-the-thickness distribution of stresses. Because of the expansion of the transverse shear and normal stresses in terms of the basis functions $\tilde{L}_i(z)$, even the first order shear and normal deformable plate theory is able to match the cubic or the parabolic distributions of the transverse normal and the transverse shear stress components. The values of these stresses are obtained from expressions (18) of the presented plate theory rather than by integrating the three-dimensional elasticity equations as is often done in the conventional third order shear deformation plate theory.

For the three antisymmetric modes of vibration, and for $mh/a = nh/b = 0.15$, we compare in Table 4 the maximum values of different stress components computed from the plate theory with those obtained from the exact solution of Srinivas and Rao [11]. These comparisons reveal that the present fifth order shear and normal deformable plate theory (5M) gives maximum values of stresses which are within 1·7% of their analytical values. The largest error occurs in the value of the transverse normal stress, and the maximum error in the other components of the stress tensor is around 0·6%. For modes I-A and II-A, the

TABLE 4

For an Aragonite crystal (orthotropic) simply supported rectangular plate, comparison of the exact maximum values of different stress components with those computed from the present fifth-order shear and normal deformable plate theory

	$\dfrac{\hat{S}_{yy}^{max}}{\hat{S}_{xx}^{max}}$	$\dfrac{\sigma^{max}}{\hat{S}_{xx}^{max}}$	$\dfrac{\hat{S}_{xy}^{max}}{\hat{S}_{xx}^{max}}$	$\dfrac{s_x^{max}}{\hat{S}_{xx}^{max}}$	$\dfrac{s_y^{max}}{\hat{S}_{xx}^{max}}$
Mode I-A					
Exact value	0·7278	0·0301	0·4759	0·2827	0·229
% error Kirchhoff	− 15·61	− 100·00	− 10·23	3·71	− 11·66
% error Mindlin	5·70	− 100·00	3·74	16·94	15·46
% error 1M	5·73	− 100·00	3·76	16·93	15·49
% error 3M	0·90	25·12	0·04	0·28	0·17
% error 5M	0·02	− 1·68	0·00	0·02	0·02
Mode II-A					
Exact value	0·0565	0·0002	0·1396	0·6128	0·5355
% error Mindlin	− 69·20	− 100·00	11·96	− 23·04	− 27·06
% error 1M	− 9·24	− 100·00	1·61	− 20·65	− 21·79
% error 3M	0·15	246·90	0·02	0·81	0·75
% error 5M	0·03	− 0·00	0·00	− 0·01	− 0·02
Mode III-A					
Exact value	0·8624	0·1657	0·5336	0·4407	1·3100
% error Mindlin	− 44·29	− 100·00	− 30·70	134·17	− 56·53
% error 1M	− 0·37	− 100·00	− 0·25	− 23·83	− 22·67
% error 3M	− 3·31	13·46	− 0·11	− 0·84	− 0·83
% error 5M	− 0·30	− 0·72	− 0·07	− 0·58	− 0·59

maximum value of the transverse normal stress is an order of magnitude smaller than that of the other components of the stress tensor. However, for mode III-A, the maximum value of σ is about one-fifth of $\hat{S}_{xx}^{max}$, although the plate studied is only moderately thick. Chao *et al.* [4] and Kant and Swaminathan [18] have not compared stresses computed from the plate theories with those obtained from the solution of the three-dimensional elasticity equations.

7. CONCLUSIONS

We have derived a Kth order shear and normal deformable plate theory by finding a saddle point of the Hellinger–Reissner functional. The three components of the displacement and the six components of the stress tensor are expanded in the thickness direction, z, by taking Legendre polynomials as basis functions for the displacements and in-plane stresses and polynomials of two degree higher for the transverse normal and the transverse shear stresses. The traction boundary conditions on the top and the bottom surfaces of the plate are exactly satisfied by the presumed stress fields. Thus, the present higher order plate theory differs from those available in the literature in two respects, namely, the transverse shear and normal stresses are expressed as polynomials in z of degree 2 higher than the displacements, and the tractions applied on the top and the bottom surfaces of the plate explicitly appear in the constitutive relations.

For a homogeneous transversely isotropic plate, we prove that the problem of plane travelling waves for every order K can be partitioned into four uncoupled simpler problems corresponding to the symmetric transverse, skewsymmetric transverse, longitudinal membranal and longitudinal flexural waves.

A complete analysis of the longitudinal membranal and flexural waves in a second order plate theory is performed and results are depicted by associating to each displacement component in the waveform a different color. Several coupling phenomena between the in-plane and through-the-thickness displacement components are found; for instance, in a given range of the dimensionless frequency, longitudinal membranal waves necessarily involve a change in thickness and a longitudinal displacement field that varies quadratically through the thickness. Since the dimensionless frequency ϖ is proportional to the plate thickness h, the range of frequency at which a given phenomenon occurs can differ considerably for thin and thick plates.

The lengths of decay of the wave solutions under quasistatic conditions are also studied. This will enable one to retain terms in the expansions for displacements that are most appropriate for the plate problem being studied. For example, from the results given in Table 2, one can conclude that for studying deformations associated with the LM waves, one can use an incomplete theory with kinematic variables U_0, U_2, W_1, U_4 and U_6, and neglect W_3 and W_5 since the waves involving W_3 and W_5 have a much smaller length of decay.

Frequencies upto the fifth mode of free vibration of a thick homogeneous orthotropic plate computed with the present fifth order, shear and normal deformable plate theory are found to match very well with those obtained from an analytical solution of the three-dimensional elasticity equations. We note that in the fourth mode of vibration symmetric about the midplane, the present third order shear and normal deformable plate theory has an error of at least 10%. These errors are reduced to less than 0·6% when a fifth order plate theory is used.

The proposed plate theory is also very accurate in evaluating the stress distributions since the fifth order plate theory has an error of at most 0·6% in the maximum values of the

transverse normal and the transverse shear stresses. These stresses are computed from the equations of the plate theory rather than by integrating the three-dimensional elasticity equations.

REFERENCES

1. R. D. MINDLIN and M. A. MEDICK 1959 *Journal of Applied Mechanics* **26**, 145–151. Extensional vibrations of elastic plates.
2. K. P. SOLDATOS and P. WATSON 1997 *Mathematics and Mechanics of Solids* **2**, 459–489. Accurate stress analysis of laminated plates combining two-dimensional theory with the exact three-dimensional solution for simply supported edges.
3. C. S. BABU and T. KANT 2000 *Journal of Thermal Stresses* **23**, 111–130. Refined higher-order finite element models for thermal buckling of laminated composites and sandwich plates.
4. C. C. CHAO, T. P. CHUNG, C. C. SHEU and J. H. TSENG 1994 *Journal of Vibration and Acoustics* **116**, 371–378. A consistent higher-order theory of laminated plates with nonlinear impact modal analysis.
5. P. C.-Y. LEE and J. D. YU 1998 *IEEE Transactions on Ultrasonics, Ferroelectrics and Frequency Control* **45**, 236–250. Governing equations of piezoelectric plates with graded properties across the thickness.
6. R. C. BATRA and S. VIDOLI 2002 *American Institute of Aeronautics and Astronautics Journal* **40**, 91–104. Higher order piezoelectric plate theory derived from a three-dimensional variational principle.
7. A. MESSINA 2001 *Journal of Sound and Vibration* **242**, 125–150. Two generalized higher order theories in free vibration studies of multilayered plates.
8. E. CARRERA 1999 *Journal of Sound and Vibration* **225**, 803–829. A study of transverse normal stress effect on vibration of multilayered plates and shells.
9. A. DI CARLO, P. PODIO-GUIDUGLI and W. O. WILLIAMS 2001 *International Journal of Solids and Structures* **38**, 1201–1225. Shells with thickness distension.
10. E. COSSERAT and F. COSSERAT 1907 *Comptes Rendus de l' Académie des Sciences* **145**, 1409–1412. Sur la statique de la ligne deformable.
11. S. SRINIVAS and A. K. RAO 1970 *International Journal of Solids and Structures* **6**, 1463–1481. Bending, vibration and buckling of simply supported thick orthotropic rectangular plates and laminates.
12. J. N. REDDY 1984 *Journal of Applied Mechanics* **51**, 745–752. A simple higher-order theory for laminated composite plates.
13. N. F. HANNA and A. W. LEISSA 1994 *Journal of Sound and Vibration* **170**, 545–555. A higher order shear deformation theory for the vibration of thick plates.
14. S. R. MARUR and T. KANT 1996 *Journal of Sound and Vibration* **194**, 337–351. Free vibration analysis of fiber reinforced composite beams using higher order theories and finite element modelling.
15. J. L. ERICKSEN 1973 *Journal of Elasticity* **3**, 161–167. Plane infinitesimal waves in homogeneous elastic plates.
16. P. C. YANG, C. H. NORRIS and Y. STARSKY 1966 *International Journal of Solids and Structures* **2**, 665–684. Elastic wave propagation in heterogeneous plates.
17. T. KANT and K. SWAMINATHAN 2001 *Journal of Sound and Vibration* **241**, 319–327. Free vibration of isotropic, orthotropic, and multilayer plates based on higther order refined theories.